

*Research Report*  
*KTC-02-13/SPR 200-99-1F*

KENTUCKY  
TRANSPORTATION  
CENTER

*College of Engineering*

FLEXURAL BEHAVIOR OF R/C  
BEAMS STRENGTHENED  
WITH CFRP SHEETS OR FABRIC



UNIVERSITY OF KENTUCKY

Research Report  
KTC-02-13/SPR 200-99-1F

# FLEXURAL BEHAVIOR OF R/C BEAMS STRENGTHENED WITH CFRP SHEETS OR FABRIC

by

**P. Alagusundaramoorthy**

Visiting Professor, Kentucky Transportation Center

**I. E. Harik**

Professor of Civil Engineering and Head, Structures Section,  
Kentucky Transportation Center

and

**C.C. Choo**

Research Student of Civil Engineering

Kentucky Transportation Center  
College of Engineering, University of Kentucky

in cooperation with

Transportation Cabinet  
Commonwealth of Kentucky

and

Federal Highway Administration  
U.S. Department of Transportation

The contents of this report reflect the views of the authors who are responsible for the facts and accuracy of the data presented herein. The contents do not necessarily reflect the official views or policies of the University of Kentucky, the Kentucky Transportation Cabinet, nor the Federal Highway Administration. This report does not constitute a standard, specification or regulation. The inclusion of manufacturer names or trade names are for identification purposes and are not to be considered as endorsement.

August 2002



Commonwealth of Kentucky  
**Transportation Cabinet**  
Frankfort, Kentucky 40622

**James C. Codell, III**  
Secretary of Transportation

**Paul E. Patton**  
Governor

**Clifford C. Linkes, P.E.**  
Deputy Secretary

August 12, 2002

Mr. Jose M. Sepulveda  
Division Administrator  
Federal Highway Administration  
330 West Broadway  
Frankfort, KY 40602

Subject: - Implementation Statement for Final Report entitled "Flexural Behavior of R/C Beams Strengthened With CFRP Sheets Or Fabric"  
- Study number: KYSPR 99-200  
- Study title: Implementation of Advanced Composites Technology for Repair and Strengthening of Kentucky Bridges.

Dear Mr. Sepulveda:

This study was conducted to investigate the feasibility of using carbon fiber reinforced polymer (CFRP) Sheets or fabric in increasing the flexural strength of concrete beams. The objective set forth has been achieved by conducting series of experiments in the Structural Engineering Laboratory at the University of Kentucky.

The behavior of concrete beams strengthened with externally bonded CFRP sheets or fabric is experimentally investigated. An analytical procedure is developed to predict the flexural behavior of concrete beams bonded with FRP sheets or fabric. Results of the testing showed that the flexural strength is increased up to 40% on beams strengthened with two layers of CFRP fabric, 49% for beams strengthened with two 1.42 mm thick CFRP sheets, and 58% on beams strengthened with two anchored 4.78 mm CFRP sheets.

Sincerely,

J. M. Yowell, P.E.  
State Highway Engineer

c: Marcie Mathews  
John Carr



**Technical Report Documentation Page**

<b>1. Report No.</b> KTC-02-13/SPR 200-99-1F	<b>2. Government Accession No.</b>	<b>3. Recipient's Catalog No.</b>	
<b>4. Title and Subtitle</b>  <b>FLEXURAL BEHAVIOR OF R/C BEAMS STRENGTHENED WITH CFRP SHEETS OR FABRIC (KYSPR 99-200)</b>		<b>5. Report Date</b> August 2002	
		<b>6. Performing Organization Code</b>	
<b>7. Author(s):</b> P. Alagusundaramoorthy, I.E. Harik, and C.C.Choo		<b>8. Performing Organization Report No.</b> KTC-02-13/SPR 200-99-1F	
<b>9. Performing Organization Name and Address</b>  Kentucky Transportation Center College of Engineering University of Kentucky Lexington, Kentucky 40506-0281		<b>10. Work Unit No. (TRAIS)</b>	
		<b>11. Contract or Grant No.</b> KYSPR 99-200	
		<b>13. Type of Report and Period Covered</b>  Final	
<b>12. Sponsoring Agency Name and Address</b>  Kentucky Transportation Cabinet State Office Building Frankfort, Kentucky 40622		<b>14. Sponsoring Agency Code</b>	
		<b>15. Supplementary Notes</b> Prepared in cooperation with the Kentucky Transportation Cabinet and the U.S. Department of Transportation, Federal Highway Administration.	
<b>16. Abstract</b>  The resistance to electro-chemical corrosion, high-strength to weight ratio, larger creep strain, fatigue resistance, non-magnetic and non-metallic properties of carbon fiber reinforced polymer (CFRP) composites offer a viable alternative to bonding of steel plates in repair and rehabilitation of reinforced concrete structures. The objective of this investigation is to study the effectiveness of externally bonded CFRP sheets or fabric in increasing the flexural strength of concrete beams. Four-point bending flexural tests are conducted up to failure on nine concrete beams strengthened with different layouts of CFRP sheets and fabric, and three beams with different layouts of anchored CFRP sheets. An analytical procedure, based on compatibility of deformations and equilibrium of forces, is presented to predict the flexural behavior of beams strengthened with FRP sheets and fabric. Comparisons are made between the test results and the analytical calculations.  Results of the testing showed that the flexural strength is increased up to 40% on beams strengthened with two layers of CFRP fabric, 49% for beams strengthened with two 1.42 mm thick CFRP sheets, and 58% on beams strengthened with two anchored 4.78 mm CFRP sheets.			
<b>17. Key Words</b> Reinforced Concrete Beams, Bending, Strengthening, CFRP Sheets and Fabric, Testing, Analysis		<b>18. Distribution Statement</b> Unlimited with approval of Kentucky Transportation Cabinet	
<b>19. Security Classif. (of this report)</b> Unclassified	<b>20. Security Classif. (of this page)</b> Unclassified	<b>21. No. of Pages</b> 42	<b>22. Price</b>

## Table of Contents

List of Tables	ii
List of Figures	iii
Notation	iv
Acknowledgments	v
1 Executive Summary	1
2 Introduction	4
3 Test Specimens	4
4 Material Properties	5
5 Bonding of CFRP Sheets	5
6 Bonding of CFRP Fabric	6
7 Test Details	6
8 Failure Pattern	7
8.1 Control Beams	7
8.2 Beams Strengthened with 76 mm wide CFRP Sheets	7
8.3 Beams Strengthened with 102 mm wide CFRP Sheets	7
8.4 Beams Strengthened with CFRP Fabric	8
9 Results and Discussion	8
9.1 Centerline Deflection at Service Load	9
9.2 Centerline Deflection at Failure Load	
9.3 Failure Load	9
9.4 Longitudinal Stress in CFRP Sheets/Fabric at Failure Load	10
10 Analytical Study	10
11 Comparison of Analytical Calculations with Experimental Results	12
12 Summary and Conclusions	12
References	34

## List of Tables

Table 1	Test Specimens	15
Table 2	Properties of CFRP Sheets, Fabric, and Epoxies	16
Table 3	Effect of Strengthening R/C Beams with CFRP Sheets on Centerline Deflection and Failure Load	17
Table 4	Effect of Strengthening R/C Beams with CFRP Fabric on Centerline Deflection and Failure Load	18
Table 5	Comparison of Analytical Calculations with, Experimental Results of R/C Beams Strengthened with CFRP Sheets	19
Table 6	Comparison of Analytical Calculations with Experimental Results of R/C Beams Strengthened with CFRP Fabric	20
Table 7	Comparison of Analytical Failure Load with Experimental Failure Load of R/C Beams Strengthened with CFRP Sheets or Fabric	21

## List of Figures

Figure 1	(a) Test Setup for Four Point Bending; (b) Reinforcement Details	22
Figure 2	CFRP Sheets Anchored to the Beam through Bolted Connections Near	23
Figure 3	(a) Position of Strain Gages; (b) Position of Linear Variable Deflection Transducers	24
Figure 4	Failure Pattern of Beams: (a) CB5-3S; (b) CB10-2SB; and (c) CB11-1F	25
Figure 5	Analytical and Experimental Load/Centerline Deflection Curves of beams Strengthened with 76 mm Wide CFRP Sheets	26
Figure 6	Analytical and Experimental Load/Deflection Curves of Beams Strengthened with 102 mm Wide CFRP Sheets.	27
Figure 7	Analytical and Experimental Load/Deflection Curves of Beams Bonded with CFRP Fabric	28
Figure 8	Load/Strain Curves on CFRP Sheets in Beam CB4-2S	29
Figure 9	Longitudinal Stress in 76 mm Wide CFRP Sheets at Failure Load	30
Figure 10	Longitudinal Stress in 102 mm Wide CFRP Sheets at Failure Load	31
Figure 11	Longitudinal Stress in CFRP Fabric at Failure Load	32
Figure 12	(a) Hognestad's Stress-Strain Model for Concrete; (b) Stress-Strain Models for Steel and CFRP Sheet/fabric; (c) Strain, Stress, and Force Diagrams; (d) Integration Model for Deflection	33

## Notation

$A_f$	= areas of FRP composites;
$A_{si}$	= area of reinforcing steel in layer $i$ ;
$b$	= width of concrete beam;
$C_c$	= concrete compressive force;
$T_c$	= concrete tensile force;
$c$	= depth of neutral axis from extreme compression fiber;
$d_i$	= distance between the extreme compression fiber to the centroid of steel in layer $i$ ;
$d_f$	= distance between the extreme compression fiber to centroid of FRP composites;
$E_s$	= modulus of elasticity of steel;
$E_f$	= modulus of elasticity of FRP composites;
$f_c$	= stress in concrete;
$f_f$	= stress in FRP composites;
$f_r$	= rupture stress of concrete;
$f_{si}$	= stress in reinforcing steel in layer $i$ ;
$f'_c$	= concrete compressive strength based on 28-day cylinder tests;
$h$	= depth of the section;
$M$	= nominal moment capacity;
$w_k$	= deflection at discrete point $k$ ;
$x$	= distance between the neutral axis to the rupture strain of concrete in tension;
$\phi_k$	= curvature at discrete point $k$ ;
$\theta_k$	= slope at discrete point $k$ .

## **Acknowledgments**

The financial support for this project was provided by the Kentucky Transportation Center, the Federal Highway Administration, and the National Science Foundation under the grant CMS- 9601674 - ARI program.

The help of Sean Anderson, Dr. Wael Zatar, Emily Delaney, Chen Denglin, Dan Eaton, Dr. Jeff Griffin, Chris Hill, Meg Hopkins, Mario Johnson, Tyler Julliard, Professor Anibal Manzelli, Dr. Vasudevan Krishnappa Naidu, Dr. Chelliah Madasamy, Johnson Joshua, David Ritchie, Laura Schweri, Robin Siddiqui, Tim Taylor, Dr. Michael Whitney, Everett Wilson, Louis Mattingly, Anthony Kordenbrock, Dr. V. Gupta and Mr. Robert Thompson at Fiber Reinforced Systems (FRS), Columbus, Ohio in coordinating, conducting the testing and preparing the manuscript is noteworthy. The authors would like to acknowledge the cooperation, suggestions, and advice of the members of the study advisory committee: Steve Goodpaster, Stuart Goodpaster, Ray Greer, Stephen Halloran and David Steele.

# 1 Executive Summary

## 1.1 Introduction

Four point bending flexural tests are conducted on two concrete control beams and twelve concrete beams strengthened with externally bonded carbon fiber reinforced polymer (CFRP) sheets/fabric. An analytical procedure, based on compatibility of deformations and equilibrium of forces, is developed. The effectiveness of externally bonded CFRP sheets or fabric on the flexural strength of concrete beams is studied. The centerline deflections at service load and at failure load, maximum strain in CFRP sheets/fabric at failure, stress variation in CFRP sheets/fabric along the span length at failure load, and failure load are calculated, and compared with experimental results. The failure load of the strengthened beams is also calculated using Whitney's stress block and compared with the presented analytical procedure.

## 1.2 Objective and Scope

The objective of this investigation is to study the effectiveness of CFRP sheets or fabric supplied by Fiber Reinforced Systems (FRS) in increasing the flexural strength of concrete beams. The objective is achieved by conducting the following tasks: (i) Flexural testing of concrete beams strengthened with different layouts of CFRP sheets or fabric; (ii) Calculating the effect of different layouts of CFRP sheets or fabric on the flexural strength; (iii) Evaluating the failure modes; (iv) Developing an analytical procedure to calculate the flexural strength of concrete beams strengthened with FRP composites; and (v) Comparing the analytical calculations with experimental results.

## 1.3 Test Specimens

Four-point bending flexural tests are conducted up to failure on two concrete control beams and twelve concrete beams strengthened with externally bonded CFRP sheets or fabric on the tension face. The pultruded CFRP sheets were provided by Fiber Reinforced Systems (FRS) in Columbus, Ohio. The CFRP fabric is a stitched unidirectional sheet of 0.18 mm thick. The length, breadth and depth ( $\ell \times b \times d$ ) of all concrete beams is kept as 4,880 mm x 230 mm x 380 mm. Each concrete beam is reinforced with two 25 mm dia. steel bars for tension and two 9 mm dia. steel bars for compression along with 9 mm dia. bars at a spacing of 150 mm center-to-center for shear reinforcement. The flexural span of all beams is kept as 4,576 mm.

The concrete control beams are designated as CB1 and CB2 respectively. Five beams strengthened with different layouts of CFRP sheets (CB3-2S, CB4-2S, CB5-3S, CB6-3S and CB7-1S), three beams strengthened with different layers of anchored CFRP sheets (CB8-1SB, CB9-1SB and CB10-2SB), and four beams strengthened with different layouts of CFRP fabric (CB11-1F, CB12-1F, CB13-2F and CB14-2F) are fabricated. For beams strengthened with bolted plates, four bolts are used at each end to anchor the CFRP sheet in beams CB8-1SB and

CB9-1SB, and eight bolts are used on each end of the sheets in beam CB10-2SB. The details of the beams fabricated for testing are presented in Table 1.1

## **1.4 Experimental Results**

The failure loads are obtained from the load/deflection curves using the “top of the knee method”. The failure load according to this method is essentially the load corresponding to the maximum load prior to load shedding. The failure loads of the beams with their corresponding failure modes are presented in Tables 1.2 and 1.3. The centerline deflection of the beams at a service load of 53 kN and at failure load is also presented in Tables 1.2 and 1.3. The average value of centerline deflections and failure load of the control beams CB1 and CB2 is calculated (Tables 1.2 and 1.3) and used as a baseline value for comparison with the strengthened beams. The percentage reduction in centerline deflection, and increase in flexural strength are calculated and presented in Tables 1.2 and 1.3.

## **1.5 Analytical Study**

An analytical procedure, based on the compatibility of deformations and equilibrium of forces, is developed to predict the flexural behavior of concrete beams strengthened with FRP composites. The following assumptions are made in the formulations: (1) Strain distribution is linear throughout the beam section; (2) shear deformation is small; (3) perfect bond between concrete surface and FRP sheets/fabric; and (4) failure of the beam occurs when either the compressive strain in concrete reaches 0.003 or the tensile strain in FRP composites reaches its ultimate strain. Hognestad’s stress-strain curve for concrete in compression is used in the analysis. The reinforcing steel is assumed to be elastic-plastic, and linear stress and strain relationship is assumed for CFRP sheets/fabric.

The centerline deflections at service load and at failure load, maximum strain in CFRP sheets/fabric at failure, stress variation in CFRP sheets/fabric along the span length at failure load, and failure load are calculated, and compared with experimental results. The comparison of analytical calculations with experimental results indicates that the analytical procedure overestimates the centerline deflections at service load and underestimates the failure load. But the predictions on centerline deflection and maximum strain in CFRP sheets/fabric at failure are in good agreement with the experimental results. Since the analytical procedure underestimates the failure load and is in good agreement with the maximum deflection and strain at failure load, it can be used for the design of concrete beams strengthened/retrofitted with CFRP sheets/fabric.

The failure load of the strengthened beams is also calculated using Whitney's stress block instead of the parabolic stress block. The maximum allowable strain in concrete is assumed to be 0.003. The failure load calculated using Whitney's stress block compares well with the failure load calculated using the more detailed analytical procedure.

## 1.6 Conclusions

The following conclusions are drawn based on the experimental and analytical studies carried out under this investigation.

- (i) The flexural strength is increased up to 49% on concrete beam strengthened with CFRP sheets.
- (ii) The flexural strength is increased up to 58% on concrete beam strengthened with anchored CFRP sheets.
- (iii) The flexural strength is increased up to 40% on concrete beam strengthened with CFRP fabric.
- (iv) The proposed analytical procedure can be used for the design of concrete beams strengthened/retrofitted with CFRP sheets/fabric.
- (v) Whitney's stress block can also be used to calculate the failure load of concrete beams strengthened with CFRP sheets/fabric.

## 2 Introduction

The technique of bonding steel plates using epoxy adhesives is recognized as an effective and convenient method for repair and rehabilitation of existing reinforced concrete structures. However the problems associated with the steel corrosion, handling due to excessive size and weight, undesirable formation of welds, partial composite action with the surface concrete and de-bonding lead to the need for alternative materials, and further research in this field. The high strength to weight ratio, resistance to electro-chemical corrosion, larger creep strain, good fatigue strength, potential for decreased installation costs and repairs due to lower weight in comparison with steel, non-magnetic and non-metallic properties of carbon fiber reinforced polymer (CFRP) composites offer a viable alternative to bonding of steel plates. The emergence of high strength epoxies has also enhanced the feasibility of using CFRP sheets and fabric for repair and rehabilitation. The flexural capacity of both prestressed and non-prestressed members may be increased through the external bonding of CFRP sheets and fabric.

An et al. (1991) and Malek et al. (1998) presented analytical procedures to calculate the flexural strength of reinforced concrete beams bonded with FRP plates. Concrete beams strengthened with externally bonded FRP strips were analyzed using the closed-form higher-order solutions by Rabinovich and Frostig (2000). The strength of concrete beams bonded with CFRP sheets (Grace et al. 1999; Spadea et al. 1998) and GFRP plates (Saadatmanesh and Ehsani 1991) was studied experimentally. The failure modes of concrete beams retrofitted with FRP materials and the techniques used in analyzing the failure modes were reviewed by Buyukozturk and Hearing (1998). The behavior of concrete beams strengthened with externally bonded FRP plates (Sharif et al. 1994; Ross et al. 1999; and Mukhopadhyaya et al. 1998) and CFRP fabric (GangaRao and Vijay 1998) was studied both experimentally and analytically. Guidelines were presented by Sonobe et al. (1997) for the design of reinforced concrete building structures using FRP composites. To date, extensive research work was conducted on the flexural strength of concrete beams bonded with various types of FRP composites.

The objective of this investigation is to study the effectiveness of CFRP sheets or fabric supplied by Fiber Reinforced Systems (FRS) in increasing the flexural strength of concrete beams. The objective is achieved by conducting the following tasks: (i) Flexural testing of concrete beams strengthened with different layouts of CFRP sheets or fabric; (ii) Calculating the effect of different layouts of CFRP sheets or fabric on the flexural strength; (iii) Evaluating the failure modes; (iv) Developing an analytical procedure to calculate the flexural strength of concrete beams strengthened with FRP composites; and (v) Comparing the analytical calculations with experimental results.

## 3 Test Specimens

Four-point bending flexural tests are conducted up to failure on two concrete control beams and twelve concrete beams strengthened with externally bonded CFRP sheets or fabric on the tension face. The pultruded CFRP sheets were provided by Fiber Reinforced Systems (FRS)

in Columbus, Ohio. The CFRP fabric is a stitched unidirectional sheet of 0.18 mm thick. The length, breadth and depth ( $\ell \times b \times d$ ) of all concrete beams is kept as 4,880 mm x 230 mm x 380 mm. Each concrete beam is reinforced with two 25 mm dia. steel bars for tension and two 9 mm dia. steel bars for compression along with 9 mm dia. bars at a spacing of 150 mm center-to-center for shear reinforcement (Fig. 1). The flexural span of all beams is kept as 4,576 mm.

The concrete control beams are designated as CB1 and CB2 respectively. Five beams strengthened with different layouts of CFRP sheets (CB3-2S, CB4-2S, CB5-3S, CB6-3S and CB7-1S), three beams strengthened with different layers of anchored CFRP sheets (CB8-1SB, CB9-1SB and CB10-2SB), and four beams strengthened with different layouts of CFRP fabric (CB11-1F, CB12-1F, CB13-2F and CB14-2F) are fabricated. For beams strengthened with bolted plates, four bolts are used at each end to anchor the CFRP sheet in beams CB8-1SB and CB9-1SB, and eight bolts are used on each end of the sheets in beam CB10-2SB (Fig. 2). The details of the beams fabricated for testing are presented in Table 1.

## 4 Material Properties

Concrete with compressive strength of 31 MPa and reinforcing steel with yield strength of 414 MPa are used. The Young's modulus ( $E_f$ ) and ultimate tensile stress ( $f_{fu}$ ) of the CFRP sheet or fabric materials are determined by conducting tension tests on three groups of coupons cut from the sheet and fabric with five coupons in each group. The coupons are cut to the size of 1016 mm x 25 mm. The coupons are tested using the 1,800 kN universal testing machine (UTM) with stress control. The rate of loading is kept as 310 MPa /minute. Load/strain curves are drawn for the average values of test results of coupons in each group. The load/strain curves are used to calculate the Young's modulus and the ultimate tensile stress of the CFRP sheets or fabric materials, and the calculated values are presented in Table 2. The properties of epoxies used for bonding the CFRP sheets and fabric are also presented in Table 2.

## 5 Bonding of CFRP Sheets

The tension face of concrete surface is made rough to a coarse sand paper texture by scarifying with a toothed grinder and cleaned with an air blower. The concrete surface is made free of all apparent moisture. The bonding surface of the CFRP sheet is made rough using fine sand papers until the matrix-rich on the surface is removed and fibers are exposed, and cleaned with acetone. A two-component epoxy primer is mixed thoroughly and applied to the concrete surface, and is allowed to dry for thirty minutes. A two-component structural epoxy paste is applied over the primer on the concrete surface and on the bonding surface of CFRP sheet using a 3 mm V-notched trowel. The CFRP sheet is installed over the concrete surface by starting at one end and by applying enough pressure to press out the excessive epoxy paste and trapped air pockets. The excessive epoxy paste is removed using a acetone rich wash cloth. The surfaces are clamped together until the epoxy paste is cured.

For Beams CB8-CB10, the strengthened CFRP sheets are also anchored to the concrete beams at the ends using specially designed force controlled expansion tip bolts. In these beams, prior to the application of epoxy primer, holes are drilled and cleaned using a vacuum cleaner. Holes are also drilled on CFRP sheets. At the time of bonding the CFRP sheets, the holes on the concrete beams are filled with structural epoxy paste using a resin injection gun. The bolts are then driven in to the beam through the holes on the CFRP sheets and tightened with nuts. Concrete beams strengthened with CFRP sheets are allowed to cure for seven days at room temperature.

## **6 Bonding of CFRP Fabric**

The tension face of the concrete surface is made rough to a coarse sand paper texture by scarifying with a toothed grinder and cleaned with an air blower. The concrete surface is made free of all apparent moisture. The bonding surface of the CFRP fabric is cleaned with acetone. A two-component epoxy primer is mixed thoroughly and applied to the concrete surface, and is allowed to dry for thirty minutes. A thick layer of two-component saturating epoxy is applied over the primer on the concrete surface using a paint roller. The CFRP fabric is rolled on the concrete surface, and pressed in to place at the center and moved towards each end. The CFRP fabric is kept tight and wrinkles free. A thick layer of saturating epoxy is applied over the CFRP fabric. The paint roller is used to remove any trapped air pockets and to work the saturating epoxy in to the fabric. After thirty minutes an additional layer of saturating epoxy is applied and the above procedure is repeated to bond additional layers of CFRP fabric. The concrete beams strengthened with CFRP fabric are allowed to cure for seven days at room temperature.

## **7 Test Details**

The test setup shown in Fig. 1(a) is used. The load is applied using two hydraulic jacks of 1,800 kN capacity. The load is transmitted through a rectangular plate (560 mm x 230 mm x 50 mm) to the beam. Hydraulic jacks having 184 mm ram and 150 mm stroke are used for testing. The top of the ram is provided with a spherical cap so that if any tilting of the plate occurs while loading, the spherical cap adjusts in such a way that only a perpendicular load is applied to the beam. A load cell is used to measure the load applied by the jacks. A rubber pad with a thickness of 13 mm is placed between the beam and the steel plate in order to minimize the abrasion between the steel plate and the beam while loading.

Electrical resistance disposable strain gages 6.35 mm long manufactured by Vishay Measurements Group, are used on the CFRP sheets and fabric. Reusable strain gages 76 mm long manufactured by Bridge Diagnostics, are used on the concrete side of the beam to measure the compressive strains. Out-of-plane deflections are measured using Linear Variable Deflection Transducers (LVDT) manufactured by Sensotec, Ohio. The position of strain gages and LVDT's are shown in Fig. 3. The beams are loaded according to the following sequences: (i) load cycle from zero to 53 kN and back to zero. The cycle is repeated five times to study the response of

the beams under cyclic loading; and (ii) load from zero to failure. The strain gages, LVDT's and load cell are connected to a data acquisition system. The data is recorded and stored in a computer at an interval of 1 sec. during loading.

## **8 Failure Pattern**

### **8.1 Control Beams**

The reinforced concrete control beams CB1 and CB2, fail due to yielding of tension steel followed by crushing of concrete at mid-span. After failure, flexural cracks are observed in the beams throughout the span length. No shear cracks are observed.

### **8.2 Beams Strengthened with 76 mm wide CFRP Sheets**

The concrete beams CB3-2S and CB4-2S strengthened with two CFRP sheets, fail due to yielding of steel followed by separation of CFRP sheets. Hereinafter the term separation implies that, at failure, the carbon sheet/fabric separated from the beam with a portion of the concrete cover attached to the sheet/fabric. Crushing of concrete is not observed in the beams. Separation of CFRP sheets takes place from the concrete surface at mid-span and extends towards the supports.

The concrete beams CB5-3S and CB6-3S strengthened with three CFRP sheets, fail due to yielding of steel followed by separation of CFRP sheets and crushing of concrete at one of the loading point. The separation of CFRP sheets initiates at mid-span and extends towards one of the supports.

After failure, flexural cracks are observed between the loading points on all four beams. Shear cracks are not observed. The separation of CFRP sheets with the concrete cover bonded to the sheet indicates the existence of strong bond between the concrete surface and CFRP sheets. At failure, a blast like sound is heard followed by load shedding in all four beams. A typical failure pattern is presented in Fig. 4(a) for beam CB5-3S.

### **8.3 Beams Strengthened with 102 mm wide CFRP Sheets**

The concrete beam CB7-1S strengthened with one CFRP sheet, fails due to yielding of steel followed by debonding of the CFRP sheet. Hereinafter the term debonding implies that, at failure, the carbon sheet/fabric separated from the resin without any concrete or resin attached to it. After failure, flexural cracks are observed between the loading points. Shear cracks are also observed between the loading points and the supports. Crushing of concrete is not observed in the beam after failure.

The concrete beams CB8-1SB and CB9-1SB strengthened with one anchored CFRP sheet, fail due to yielding of steel followed by debonding of the CFRP sheet and crushing of concrete at one of the loading points. In each beam, debonding of the CFRP sheet initiated at support A, and the bolts remained intact at both supports. After failure, flexural cracks are observed between the loading points. Shear cracks are not observed.

The concrete beam CB10-2SB strengthened with two anchored CFRP sheets, fails due to yielding of steel followed by debonding of the CFRP sheets, and crushing of concrete near to one of the loading point. The failure pattern of beam CB10-2SB is shown in Fig. 4(b). After failure, flexural cracks are observed between the loading points. Shear cracks are also observed between the loading points and the supports.

#### **8.4 Beams Strengthened with CFRP Fabric**

The concrete beams CB11-1F and CB12-1F strengthened with one layer of CFRP fabric, fail due to yielding of steel followed by rupture of fabric and crushing of concrete at mid-span. After failure, flexural cracks are observed in the beams. Shear cracks are not observed. The failure pattern of beam CB11-1F is shown in Fig. 4(c).

The concrete beam CB13-2F strengthened with two layers of CFRP fabric, fails due to yielding of steel followed by debonding of fabric at mid-span followed by crushing of concrete at one of the loading points. After failure, flexural cracks are observed in the beam. Shear cracks are not observed.

The concrete beam CB14-2F strengthened with two layers of CFRP fabric, fails due to yielding of steel followed by debonding of fabric near to the mid-span. After failure, flexural cracks are observed between the loading points. Shear cracks are observed between the loading points and the supports. Crushing of concrete is not observed.

After failure, the CFRP fabric is easily peeled off from all four beams, and no concrete chunks stuck to the fabric.

### **9 Results and Discussion**

The experimental load/centerline deflection curves for the beams strengthened with 76 mm wide CFRP sheets (CB3-2S, CB4-2S, CB5-3S and CB6-3S), 102 mm wide CFRP sheets (CB7-1S, CB8-1SB, CB9-1SB and CB10-2SB), and CFRP fabric (CB11-1F, CB12-1F, CB13-2F and CB14-2F) are shown in Figs. 4, 5, and 6 respectively. For comparison, the experimental load/centerline deflection curves of the control beams CB1 and CB2 are also plotted in Figs. 5, 6 and 7. The typical load/strain curves for beam CB4-2S is shown in Fig. 8.

The failure loads are obtained from the load/deflection curves using the “top of the knee method”. The failure load according to this method is essentially the load corresponding to the

maximum load prior to load shedding. The failure loads of the beams with their corresponding failure modes are presented in Tables 3 and 4. The centerline deflection of the beams at a service load of 53 kN and at failure load is also presented in Tables 3 and 4. The average value of centerline deflections and failure load of the control beams CB1 and CB2 is calculated (Tables 3 and 4) and used as a baseline value for comparison with the strengthened beams. The percentage reduction in centerline deflection, and increase in flexural strength are calculated and presented in Tables 3 and 4.

### **9.1 Centerline Deflection at Service Load**

The centerline deflection at a service load of 53 kN (Tables 3 and 4) reduces from 19% to 27% on beams strengthened with two 76 mm wide and 1.40 mm thick ( $b_s/t_s = 109$ ) CFRP sheets, 24% to 29% on beams strengthened with three 76 mm width and 1.40 mm thick ( $b_s/t_s = 163$ ) CFRP sheets, 1% to 49% on beams strengthened with one anchored 102 mm width and 4.78 mm thick ( $b_s/t_s = 21$ ) CFRP sheet, 19 % on beam strengthened with two sheets 102 mm width and 4.78 mm thick ( $b_s/t_s = 43$ ) anchored CFRP, 16 % on beam strengthened with one layer of CFRP fabric, and 24% to 27% on beams strengthened with two layers of CFRP fabric.

### **9.2 Centerline Deflection at Failure Load**

The centerline deflection at failure load (Tables 3 and 4) reduces from 5% to 17% on beams strengthened with two 76 mm width and 1.40 mm thick ( $b_s/t_s = 109$ ) CFRP sheets, 12% to 24% on beams strengthened with three 76 mm width and 1.40 mm thick ( $b_s/t_s = 163$ ) CFRP sheets, 13% to 25% on beams strengthened with one anchored 102 mm width and 4.78 mm thick ( $b_s/t_s = 21$ ) CFRP sheet, 15 % on beam strengthened with two anchored 102 mm width and 4.78 mm thick ( $b_s/t_s = 43$ ) CFRP sheets, 12% to 20% on beams strengthened with one layer CFRP fabric, and 10% to 21% on beams strengthened with two layers of CFRP fabric.

### **9.3 Failure Load**

The failure load increases from 35% to 36% on beams strengthened with two 76 mm wide and 1.40 mm thick ( $b_s/t_s = 109$ ) CFRP sheets, 42% to 49% on beams strengthened with three 76 mm wide and 1.40 mm thick ( $b_s/t_s = 163$ ) CFRP sheets. 29% to 41% on beams strengthened with one 102 mm wide and 4.78 mm thick ( $b_s/t_s = 21$ ) anchored CFRP sheet, 58 % on beam strengthened with two of 102 mm wide and 4.78 mm thick ( $b_s/t_s = 43$ ) anchored CFRP sheets, 13 % to 15% on beams strengthened with one layer of CFRP fabric, and 36% to 40% on beams strengthened with two layers of CFRP fabric.

The strength of concrete beams cannot be increased uniformly by simply adding the CFRP sheets/fabric. The plate slenderness ratio of CFRP sheets  $b_s/t_s$  and  $b_f/t_f$  of CFRP fabric are to be optimized for maximum strength.

## 9.4 Longitudinal Stress in CFRP Sheets/Fabric at Failure Load

Figs. 8, 9, and 10 show the longitudinal stress at failure load in the CFRP sheets/fabric along the span length of beams CB3-CB14. The pattern of the graphs indicates the existence of proper bond between the CFRP sheets/fabric and the concrete surface. The maximum stress at failure is 978 MPa in the 76 mm wide CFRP sheets, compared to the ultimate tensile stress of 2,068 MPa. The maximum stress at failure is 321 MPa in the 102 mm wide CFRP sheets, compared to the ultimate tensile stress of 552 MPa. The maximum stress at failure is 405 N/mm in the one layer of CFRP fabric, and 606 N/mm in the two layers of CFRP fabric (equivalent of 303 N/mm per layer).

## 10 Analytical Study

An analytical procedure, based on the compatibility of deformations and equilibrium of forces, is developed to predict the flexural behavior of concrete beams strengthened with FRP composites. The following assumptions are made in the formulations: (1) Strain distribution is linear throughout the beam section; (2) shear deformation is small; (3) perfect bond between concrete surface and FRP sheets/fabric; and (4) failure of the beam occurs when either the compressive strain in concrete reaches 0.003 or the tensile strain in FRP composites reaches its ultimate strain. Hognestad's stress-strain curve for concrete in compression as shown in Fig. 12(a) is used in the analysis (Park and Paulay 1975). The reinforcing steel is assumed to be elastic-plastic, and linear stress and strain relationship is assumed for CFRP sheets/fabric as shown in Fig. 12(b).

The compressive force  $C_c$  in concrete is expressed in terms of a parameter  $k_1$  (Park and Paulay 1975) as;

$$C_c = k_1 f_c'' bc \quad (1)$$

in which  $k_1$  is a parameter used to convert the nonlinear stress-strain relationship of concrete into an equivalent rectangular stress block,  $f_c'' = 0.9 f_c'$  in which  $f_c'$  is the design strength of concrete,  $b$  is the width of the beam section, and  $c$  is the distance between the location of the neutral axis and the extreme fiber of concrete in compression. The tensile force  $T_c$  in concrete is obtained by assuming the linear stress-strain distribution as;

$$T_c = f_r b x \quad (2)$$

in which  $f_r$  is the rupture stress of concrete, and  $x$  is the distance from the neutral axis to the rupture strain in concrete. The location of the neutral axis  $c$  is obtained by solving the equilibrium of internal forces (Eqn. 3).

$$k_1 f_c b c + f_r b x + \sum_{i=1}^n f_{si} A_{si} + \sum_{j=1}^m f_{fj} A_{fj} = 0 \quad (3)$$

in which  $f_s$  is the stress in steel,  $f_f$  stress in FRP composites,  $A_s$  is the area of steel and  $A_f$  is the area of FRP sheet or fabric.

The nominal moment carrying capacity of a section shown in Fig. 12(c) is obtained by summing the moments of all internal forces about mid-depth of the beam;

$$M = C_c \left( \frac{h}{2} - k_2 c \right) + T_c \left[ \frac{h}{2} - \left( \frac{2}{3} x + c \right) \right] + \sum_{i=1}^n f_{si} A_{si} \left( \frac{h}{2} - d_i \right) + \sum_{j=1}^m f_{fj} A_{fj} \left( \frac{h}{2} - d_{fj} \right) \quad (4)$$

in which  $h$  is the depth of the section,  $k_1$  and  $k_2$  are the parameters defined (Park and Paulay 1975),  $d_i$  is the distance between the extreme concrete compressive fiber to the centroid of steel in layer  $i$ , and  $d_f$  is the distance between the extreme concrete compressive fiber to the centroid of FRP composites.

The curvature of a section is calculated as;

$$\phi = \frac{\epsilon_c}{c} \quad (5)$$

The load/deflection response is calculated using the numerical integration technique (Chen and Atsuta 1976). The computation starts from one end of the beam at which the deflection  $w_0$ , curvature  $\phi_0$  and moment are known as zero [Fig. 12(d)]. The deflection  $w_k$ , slope  $\theta_k$ , and curvature  $\phi_k$  at point  $x_k$  on the beam are computed for a prescribed (assumed) initial slope  $\theta_0$  at the left end. The deflection of the beam is approximated as;

$$w_k = w_{k-1} + \theta_{k-1} (x_k - x_{k-1}) - \frac{1}{2} \phi_{k-1} (x_k - x_{k-1})^2 \quad (6)$$

in which the curvature  $\phi_k = f(M_k)$  is obtained from M- $\phi$  relationship for the cross section. The slope  $\theta_k$  is calculated as;

$$\theta_k = \theta_{k-1} - \phi_k (x_k - x_{k-1}) \quad (7)$$

The above procedure is repeated for the discrete points until the slope  $\theta_i$  at mid-span becomes zero. The half span of the beam is modeled into ten segments in the analysis.

## **11 Comparison of Analytical Calculations with Experimental Results**

The load/centerline deflection response of all tested beams is calculated using the analytical procedure and compared with experimental results (Figs. 5, 6 and 7). The centerline deflections at service load of 53 kN and at failure load, and maximum strain in CFRP sheets/fabric at failure load, and failure load are calculated and presented in Tables 5, 6 and 7.

The comparison of analytical calculations with experimental results indicates that the analytical procedure overestimates the centerline deflections at service load and underestimates the failure load. But the predictions on centerline deflection and maximum strain in CFRP sheets/fabric at failure are in good agreement with the experimental results.

The variation of longitudinal stress in CFRP sheets/fabric at failure load along the span length is also calculated and compared with the experimental results (Figs. 9, 10, and 11). The pattern of the curves indicate that the prediction of stresses along the span length by the analytical model is in good agreement with experimental results except for the concrete beams strengthened with one 102 mm wide and 4.78mm thick CFRP sheet.

Since the analytical procedure underestimates the failure load and is in good agreement with the maximum deflection and strain at failure load, it can be used for the design of concrete beams strengthened/retrofitted with CFRP sheets/fabric.

The failure load of the strengthened beams is also calculated using Whitney's stress block (Nawy 1996) instead of the parabolic stress block in Fig. 12(c). The maximum allowable strain in concrete is assumed to be 0.003. The failure load calculated using Whitney's stress block (Table 7) compares well with the failure load calculated using the more detailed analytical procedure.

## **12 Summary and Conclusions**

Four point bending flexural tests are conducted on two concrete control beams and twelve concrete beams strengthened with externally bonded carbon fiber reinforced polymer (CFRP) sheets/fabric. An analytical procedure, based on compatibility of deformations and equilibrium of forces, is presented. The effectiveness of externally bonded CFRP sheets or fabric on the flexural strength of concrete beams is studied. The centerline deflections at service load and at failure load, maximum strain in CFRP sheets/fabric at failure, stress variation in CFRP sheets/fabric along the span length at failure load, and failure load are calculated, and compared with experimental results. The failure load of the strengthened beams is also calculated using Whitney's stress block and compared with the presented analytical procedure.

The following conclusions are drawn based on the experimental and analytical studies carried out under this investigation.

- (vi) The flexural strength is increased up to 49% on concrete beam strengthened with CFRP sheets.
- (vii) The flexural strength is increased up to 58% on concrete beam strengthened with anchored CFRP sheets.
- (viii) The flexural strength is increased up to 40% on concrete beam strengthened with CFRP fabric.
- (ix) The proposed analytical procedure can be used for the design of concrete beams strengthened/retrofitted with CFRP sheets/fabric.
- (x) Whitney's stress block can also be used to calculate the failure load of concrete beams strengthened with CFRP sheets/fabric.

## **Tables and Figures**

**Table 1: Test Specimens**

Specimen	Beam Size			Effective span (mm)	STRENGTHENING DETAILS			
	<i>l</i> (mm)	<i>b</i> (mm)	<i>d</i> (mm)		Number of CFRP sheets/fabric <sup>2</sup>	Size of CFRP Sheet/Fabric		
						Length (mm)	Width (mm)	Thickness (mm)
CB1 <sup>1</sup>	4880	230	380	4576	-	-	-	-
CB2 <sup>1</sup>	4880	230	380	4576	-	-	-	-
CB3-2S	4880	230	380	4576	2S	4270	76	1.40
CB4-2S	4880	230	380	4576	2S	4270	76	1.40
CB5-3S	4880	230	380	4576	3S	4270	76	1.40
CB6-3S	4880	230	380	4576	3S	4270	76	1.40
CB7-1S	4880	230	380	4576	1S	4270	102	4.78
CB8-1SB	4880	230	380	4576	1SB	4270	102	4.78
CB9-1SB	4880	230	380	4576	1SB	4270	102	4.78
CB10-2SB	4880	230	380	4576	2SB	4270	102	4.78
CB11-1F	4880	230	380	4576	1F	4370	203	0.18
CB12-1F	4880	230	380	4576	1F	4370	203	0.18
CB13-2F	4880	230	380	4576	2F	4370	203	0.18
CB14-2F	4880	230	380	4576	2F	4370	203	0.18

<sup>1</sup> CB1 and CB2 are the control (or baseline) reinforced concrete beams

<sup>2</sup> # S - Number of CFRP sheets

# SB - Number of CFRP sheets with bolted connections near the supports

# F - Number of layers of CFRP fabric

**Table 2: Properties of CFRP Sheets, Fabric, and Epoxies**

Material	Properties				
	Width (mm)	Thickness (mm)	Ultimate tensile stress $f_{fu}$	Young's modulus $E_{fu}$ (GPa)	Ultimate strain $\epsilon_{fu}$ (%)
CFRP sheet	76	1.40	2,068 MPa	138	1.50
CFRP sheet	102	4.78	552 MPa	48	1.10
CFRP fabric	203	0.18	490 N/mm	228	1.80
Material	Properties				
	Tensile strength (MPa)	Adhesion (MPa)	Flexural strength (MPa)	Flexural modulus (MPa)	
Structural epoxy	61	> 2	100	2,140	
Saturating epoxy	62	> 2	103	2,400	

**Table 3: Effect of Strengthening R/C Beams with CFRP Sheets on Centerline Deflection and Failure Load**

Beam series	Specimen	CENTRELINE DEFLECTION				Load		Mode of failure <sup>5</sup>
		At service load <sup>2</sup> $\delta_{se}$ (mm)	At failure load $\delta_{ue}$ (mm)	% Reduction in Deflection <sup>3</sup>		Failure load $P_{ue}$ (kN)	% Increase in failure load <sup>4</sup>	
				At service load	At failure load			
Control beams	CB1	6.477	58.877	-	-	196	-	Yielding of steel followed by crushing of concrete
	CB2	5.664	52.375	-	-	190	-	Yielding of steel followed by crushing of concrete
	Baseline <sup>1</sup>	6.071	55.626	-	-	193	-	-
Beams strengthened with 1.40 mm thick CFRP sheets	CB3-2S	4.420	46.126	27	17	263	36	Yielding of steel followed by separation of CFRP sheets
	CB4-2S	4.928	52.807	19	5	260	35	Yielding of steel followed by separation of CFRP sheets
	CB5-3S	4.597	48.717	24	12	287	49	Yielding of steel followed by separation of CFRP sheets and crushing of concrete
	CB6-3S	4.293	42.469	29	24	275	42	Yielding of steel followed by separation of CFRP sheets and crushing of concrete
Beams strengthened with 4.78 mm thick CFRP sheets	CB7-1S	4.724	44.323	22	20	256	33	Yielding of steel followed by debonding of CFRP sheet
	CB8-1SB	3.073	41.808	49	25	273	41	Yielding of steel followed by debonding of CFRP sheet and crushing of concrete
	CB9-1SB	5.994	48.336	1	13	249	29	Yielding of steel followed by debonding of CFRP sheet and crushing of concrete
	CB10-2SB	4.928	47.498	19	15	306	58	Yielding of steel followed by separation of CFRP sheets and crushing of concrete

<sup>1</sup> The average values of CB1 and CB2 are used as baseline

<sup>2</sup> Service load = 53 kN

<sup>3</sup> % Reduction in deflection =  $\frac{\text{Deflection of baseline beam} - \text{Deflection of strengthened beam}}{\text{Deflection of baseline beam}}$

<sup>4</sup> % Increase in strength =  $\frac{\text{Failure load of strengthened beam} - \text{Failure load of baseline beam}}{\text{Failure load of baseline beam}}$

**Table 4: Effect of Strengthening R/C Beams with CFRP Fabric on Centerline Deflection and Failure Load**

Beam series	Specimen	CENTERLINE DEFLECTION				Load		Mode of failure
		At service load <sup>2</sup> $\delta_{se}$ (mm)	At failure load $\delta_{ue}$ (mm)	% Reduction in Deflection <sup>3</sup>		Failure load $P_{ue}$ (kN)	% Increase in failure load <sup>4</sup>	
				At service load	At failure load			
Control beams	CB1	6.477	58.877	-	-	196	-	Yielding of steel followed by crushing of concrete
	CB2	5.664	52.375	-	-	190	-	Yielding of steel followed by crushing of concrete
	Baseline <sup>1</sup>	6.071	55.626	-	-	193	-	-
Beams strengthened with 0.18 mm thick CFRP fabric	CB11-1F	6.350	44.628	- <sup>5</sup>	20	219	13	Rupture of CFRP fabric at mid-span followed by crushing of concrete
	CB12-1F	5.105	49.124	16	12	223	15	Rupture of CFRP fabric at mid-span followed by crushing of concrete
	CB13-2F	4.623	50.038	24	10	263	36	Debonding of CFRP fabric followed by crushing of concrete
	CB14-2F	4.420	43.790	27	21	270	40	Debonding of CFRP fabric at mid-span.

<sup>1</sup> The average values of CB1 and CB2 are used as baseline

<sup>2</sup> Service load = 53 kN

<sup>3</sup> % Reduction in deflection =  $\frac{\text{Deflection of baseline beam} - \text{Deflection of strengthened beam}}{\text{Deflection of baseline beam}}$

<sup>4</sup> % Increase in strength =  $\frac{\text{Failure load of strengthened beam} - \text{Failure load of baseline beam}}{\text{Failure load of baseline beam}}$

<sup>5</sup> Deflection at service load for beam CB11-1F is 5% greater than the baseline beam

$P_{ue}$  – Experimental failure load,  $\delta_{se}$  – Experimental deflection at service load, and  $\delta_{ue}$  – Experimental deflection at failure load

**Table 5: Comparison of Analytical Calculations with Experimental Results of R/C Beams Strengthened with CFRP Sheets**

Beam series	Specimen	CENTERLINE DEFLECTION <sup>1</sup>						Maximum Strain in CFRP Sheet at Failure <sup>2</sup>		
		At Service Load			At Failure Load			$\epsilon_a$	$\epsilon_e$	$\frac{\epsilon_e}{\epsilon_a}$
		$\delta_{sa}$ (mm)	$\delta_{se}$ (mm)	$\frac{\delta_{se}}{\delta_{sa}}$	$\delta_{ua}$ (mm)	$\delta_{ue}$ (mm)	$\frac{\delta_{ue}}{\delta_{ua}}$			
Control beams	CB1	7.696	6.477	0.84	60.38	58.88	0.98	-	-	-
	CB2	7.696	5.664	0.74	60.38	52.37	0.87	-	-	-
Beams strengthened with 1.40 mm thick CFRP sheets	CB3-2S	7.315	4.420	0.60	47.75	46.13	0.97	0.00680	0.00648	0.95
	CB4-2S	7.315	4.928	0.67	47.75	52.81	1.11	0.00680	0.00709	1.04
	CB5-3S	6.883	4.597	0.67	43.94	48.72	1.11	0.00589	0.00593	1.01
	CB6-3S	6.883	4.293	0.62	43.94	42.47	0.97	0.00589	0.00501	0.85
Beams strengthened with 4.78 mm thick CFRP sheets	CB7-1S	7.493	4.724	0.63	49.66	44.32	0.89	0.00738	0.00585	0.79
	CB8-1SB	7.493	3.073	0.41	49.66	41.81	0.84	0.00738	0.00573	0.78
	CB9-1SB	7.493	5.994	0.80	49.66	48.34	0.97	0.00738	0.00665	0.90
	CB10-2SB	6.782	4.928	0.73	44.00	47.50	1.08	0.00578	0.00600	1.04

<sup>1</sup> $\delta_{sa}$  - Analytical deflection at service load of 53 kN  
 $\delta_{se}$  - Experimental deflection at service load of 53 kN  
 $\delta_{ua}$  - Analytical deflection at failure load  
 $\delta_{ue}$  - Experimental deflection at failure load

<sup>2</sup> $\epsilon_a$  - Maximum strain in CFRP sheet at failure load from analytical study  
 $\epsilon_e$  - Maximum strain in CFRP sheet at failure load from experimental study

**Table 6: Comparison of Analytical Calculations with Experimental Results of R/C Beams Strengthened with CFRP Fabric**

Beam series	Specimen	CENTERLINE DEFLECTION <sup>1</sup>						Maximum Strain in CFRP Fabric at Failure <sup>2</sup>		
		At Service Load			At Failure Load			$\epsilon_a$	$\epsilon_e$	$\frac{\epsilon_e}{\epsilon_a}$
		$\delta_{sa}$ (mm)	$\delta_{se}$ (mm)	$\frac{\delta_{se}}{\delta_{sa}}$	$\delta_{ua}$ (mm)	$\delta_{ue}$ (mm)	$\frac{\delta_{ue}}{\delta_{ua}}$			
Control beams	CB1	7.696	6.477	0.84	60.38	58.88	0.98	-	-	-
	CB2	7.696	5.664	0.74	60.38	52.37	0.87	-	-	-
Beams strengthened with 0.18 mm thick CFRP fabric	CB11-1F	8.103	6.350	0.78	54.76	44.63	0.81	0.009301	0.009998	1.07
	CB12-1F	8.103	5.105	0.63	54.76	49.12	0.90	0.009301	0.007379	0.79
	CB13-2F	7.772	4.623	0.59	52.22	50.04	0.96	0.008130	0.007496	0.92
	CB14-2F	7.772	4.420	0.57	52.22	43.79	0.84	0.008130	0.004531	0.56

<sup>1</sup> $\delta_{sa}$  - Analytical deflection at service load of 53 kN

$\delta_{se}$  - Experimental deflection at service load of 53 kN

$\delta_{ua}$  - Analytical deflection at failure load

$\delta_{ue}$  - Experimental deflection at failure load

<sup>2</sup> $\epsilon_a$  - Maximum strain in CFRP fabric at failure load from analytical study

$\epsilon_e$  - Maximum strain in CFRP fabric at failure load from experimental study

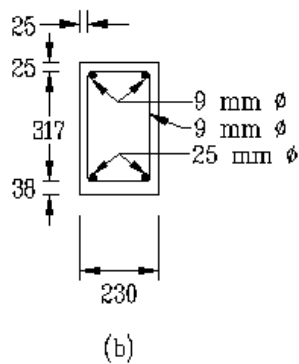
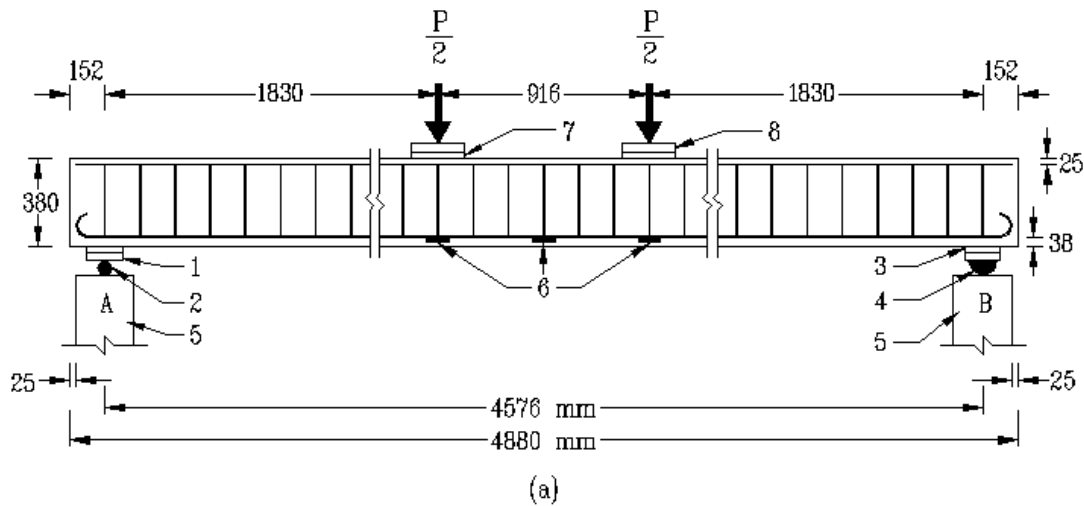
**Table 7: Comparison of Analytical Failure Load with Experimental Failure Load of R/C Beams Strengthened with CFRP Sheets or Fabric**

Specimen	Failure Load				
	$P_{ue}^1$ (kN)	$P_{uaH}^2$ (kN)	$\frac{P_{ue}}{P_{uaH}}$	$P_{uaW}^3$ (kN)	$\frac{P_{ue}}{P_{uaW}}$
CB1	196	139	1.41	139	1.39
CB2	190	139	1.37	139	1.37
CB3-2S	263	206	1.28	207	1.27
CB4-2S	260	206	1.26	207	1.26
CB5-3S	287	224	1.28	227	1.26
CB6-3S	275	224	1.23	227	1.21
CB7-1S	256	198	1.30	203	1.26
CB8-1SB	273	198	1.38	203	1.34
CB9-1SB	249	198	1.26	203	1.23
CB10-2SB	306	228	1.34	230	1.33
CB11-1F	219	165	1.33	166	1.32
CB12-1F	223	165	1.35	166	1.34
CB13-2F	263	185	1.43	185	1.43
CB14-2F	270	185	1.46	185	1.46

<sup>1</sup> $P_{ue}$  – Experimental failure load

<sup>2</sup> $P_{uaH}$  – Analytical failure load using Hognestad's stress-strain curve

<sup>3</sup> $P_{uaW}$  – Analytical failure load using Whitney's stress block



All dimensions are in mm.

1. 560 mm x 152 mm x 25 mm A36 Steel plate
2. 64 mm dia. A36 Solid steel plate
3. 560 mm x 152 mm x 13 mm Rubber pad
4. 128 mm dia. A36 Solid steel half round
5. Supporting members
6. Strain gages on steel rebars
7. 560 mm x 230 mm x 13 mm Rubber pad
8. 560 mm x 230 mm x 51 mm A36 Steel plate

**Figure 1: (a) Test Setup for Four Point Bending;  
(b) Reinforcement Details**

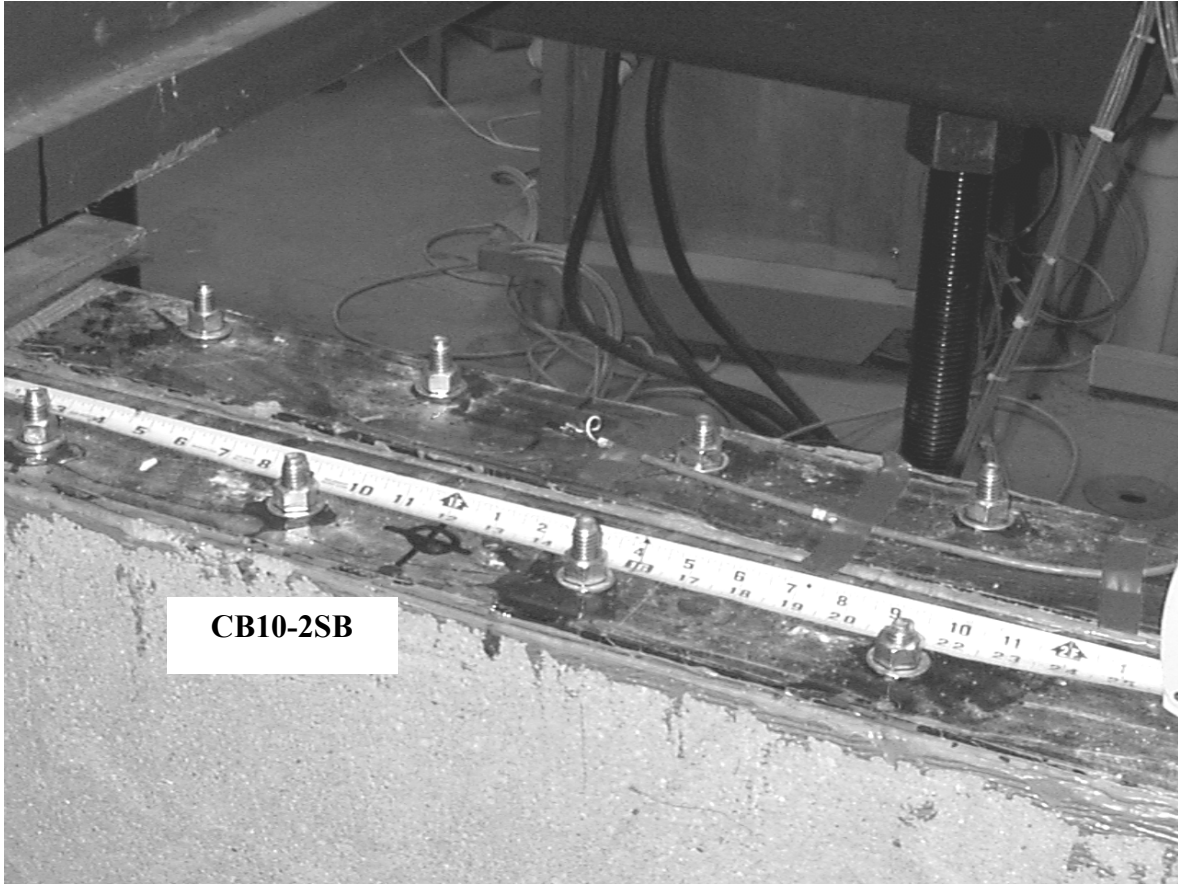
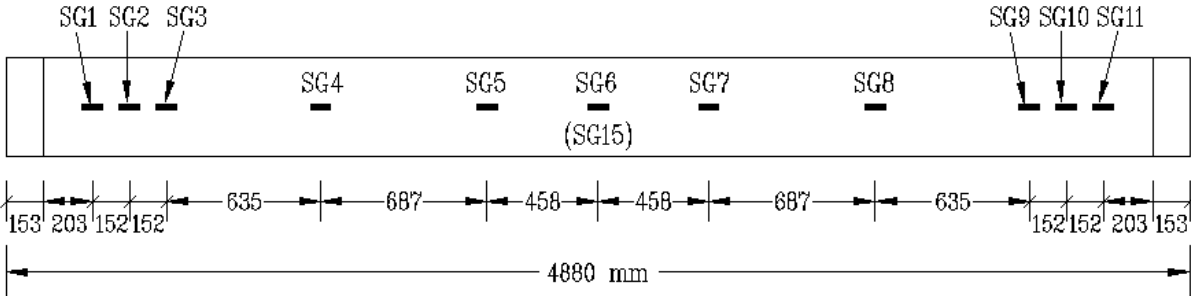
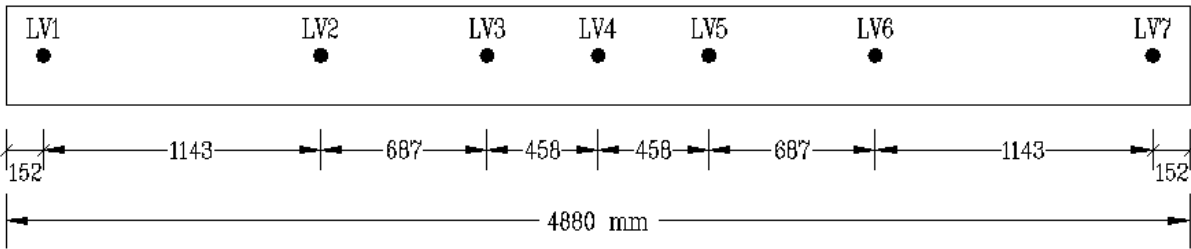


**Figure 2: CFRP Sheets Anchored to the Beam through Bolted Connections**



(a)

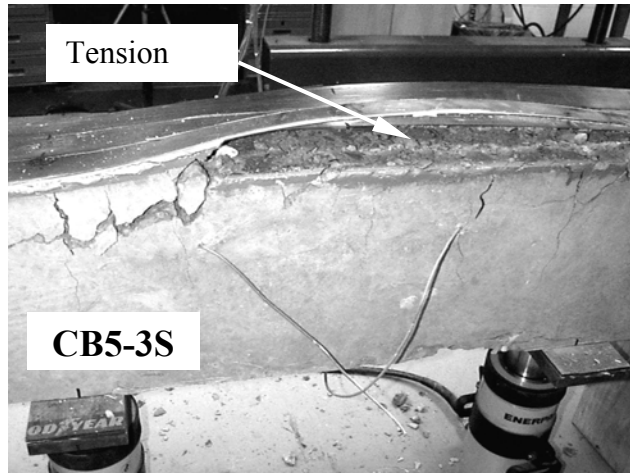


(b)

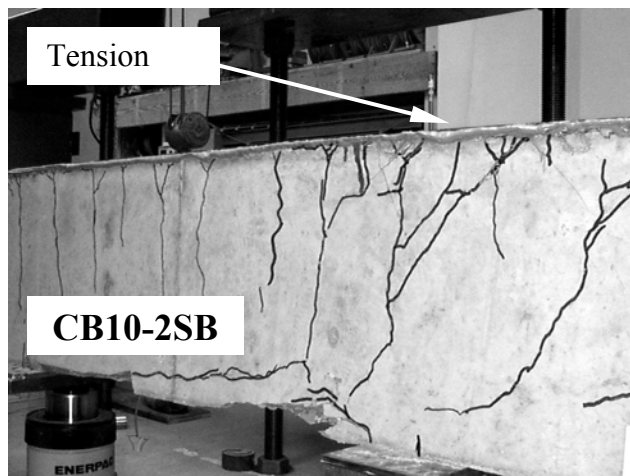
All dimensions are in mm.

- Strain gages SG1 to SG11 are located on carbon sheets
- Strain gages SG12 to SG14 are located on steel rebars
- Strain gage SG15 is located on concrete on the compression side
- LVDT's LV3 & LV5 are located at the load points

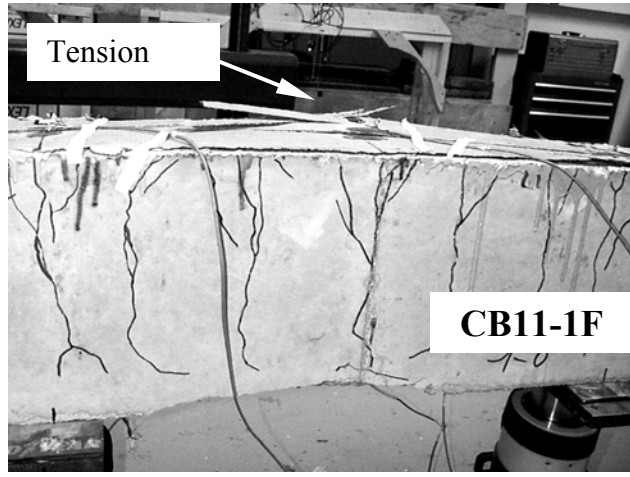
**Figure 3: (a) Position of Strain Gages; (b) Position of Linear Variable Deflection Transducers**



(a)



(b)



(c)

**Figure 4: Failure Pattern of Beams: (a) CB5-3S; (b) CB10-2SB; and (c) CB11-1F**

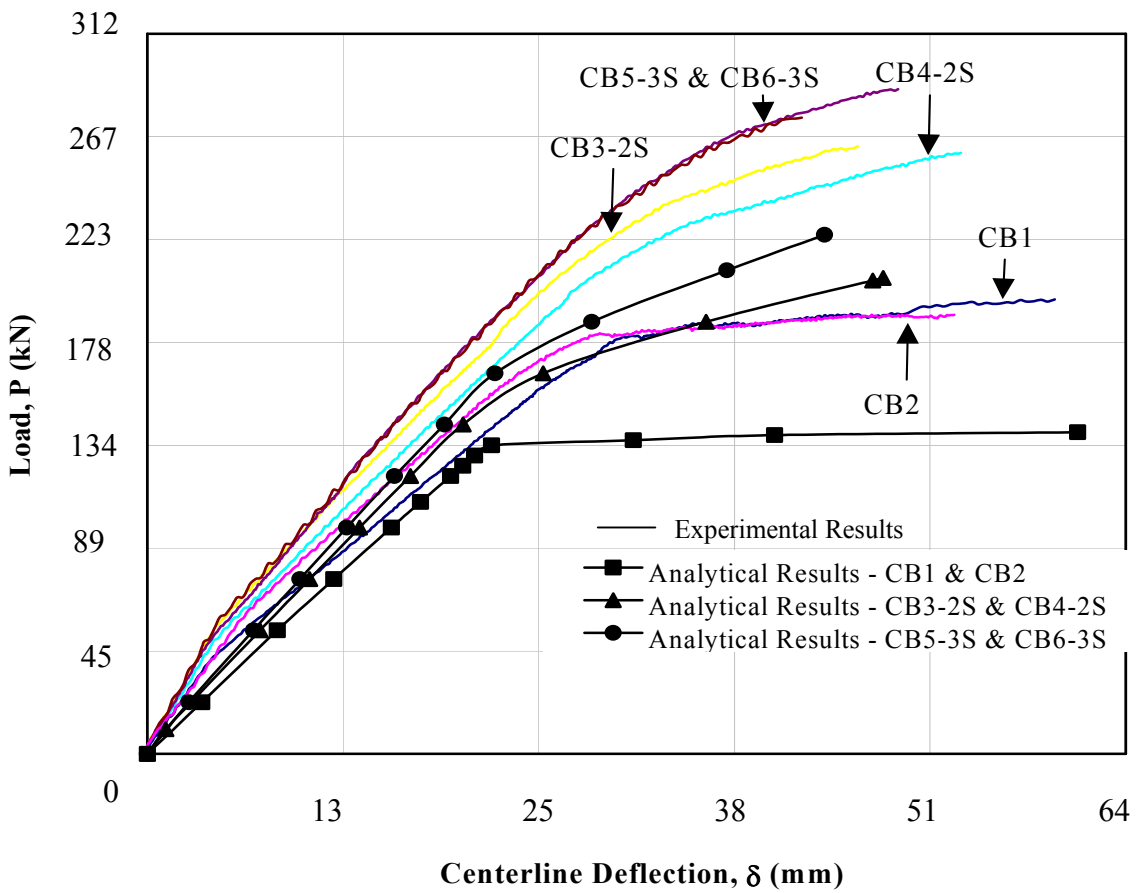


**Figure 5: Analytical and Experimental Load/Centerline Deflection Curves of beams Strengthened with 76 mm Wide CFRP Sheets**

(Refer to Table 1 for specimen identification, and Table 2 for CFRP sheet)

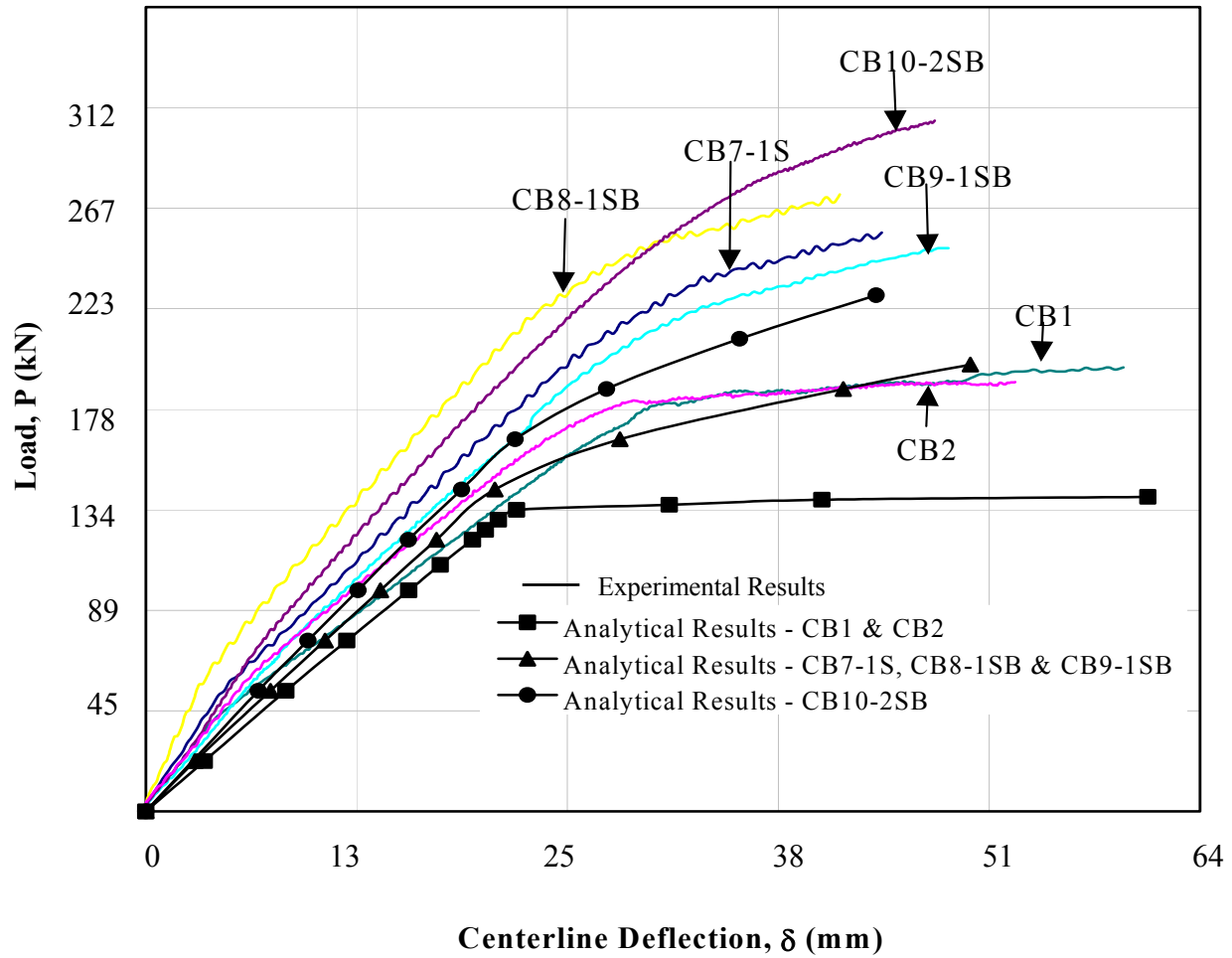


**Figure 6: Analytical and Experimental Load/Deflection Curves of Beams Strengthened with 102 mm Wide CFRP Sheets.**

(Refer to Table 1 for specimen identification, and Table 2 for CFRP sheet properties)

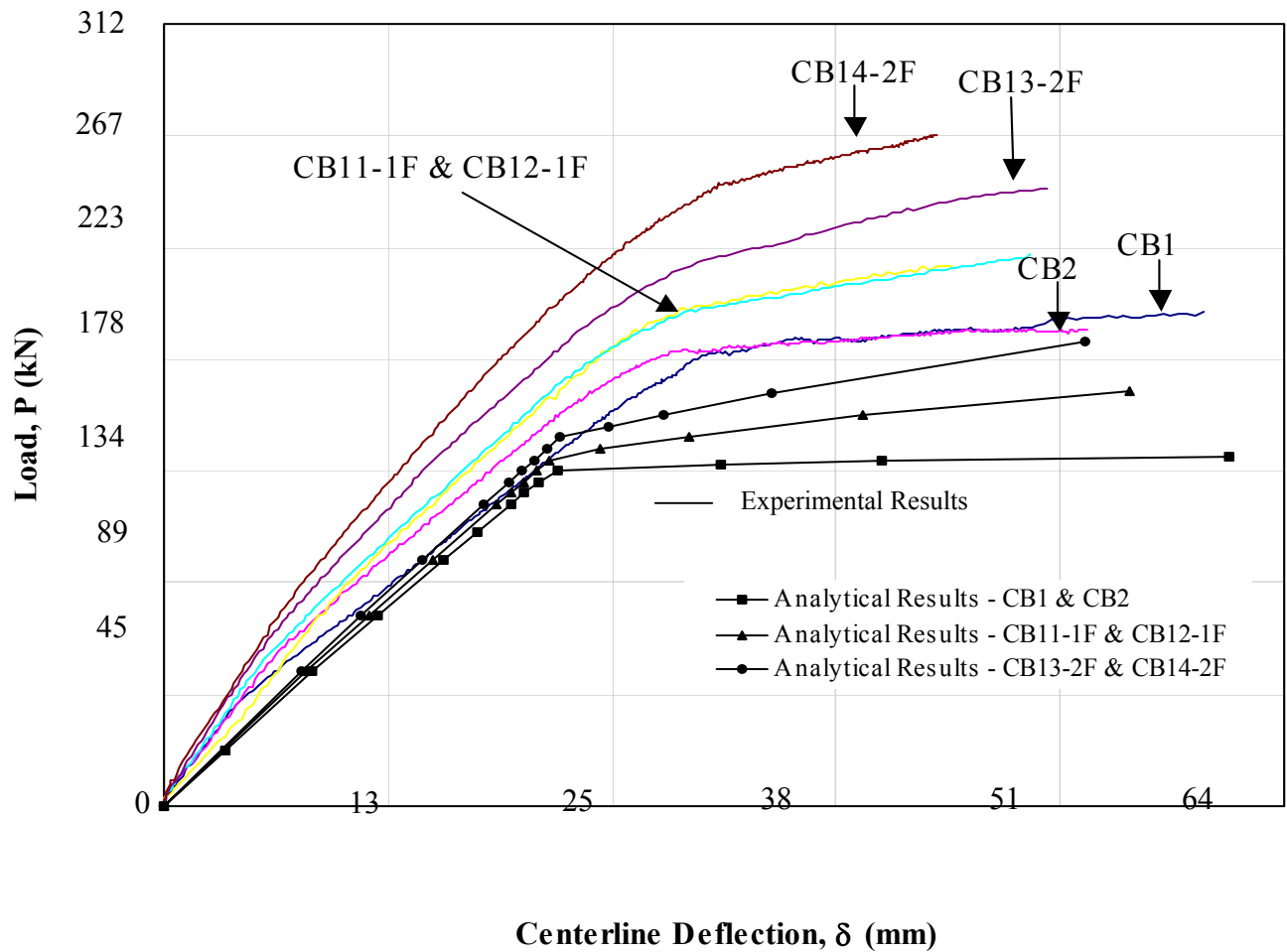


**Figure 7: Analytical and Experimental Load/Deflection Curves of Beams Bonded with CFRP Fabric**

(Refer to Table 1 for specimen identification, and Table 2 for CFRP fabric properties)

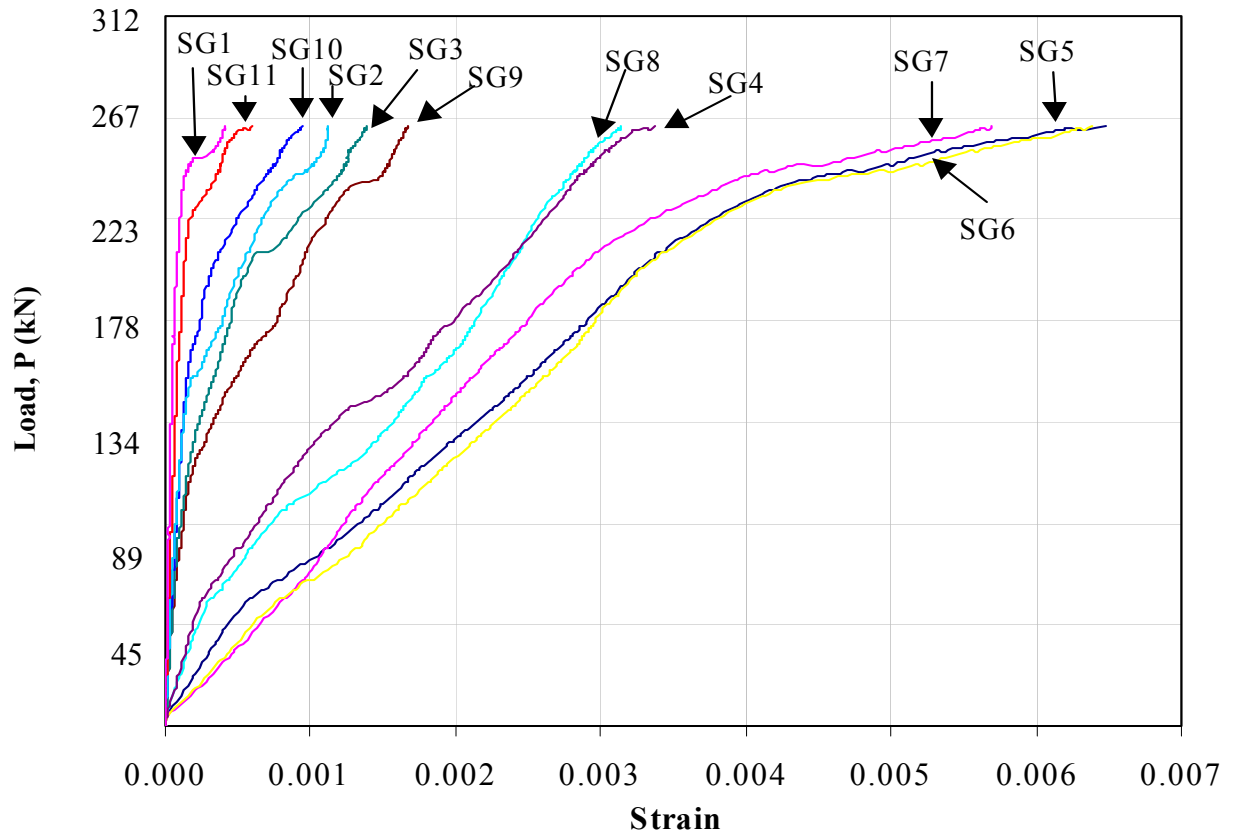


**Figure 8: Load/Strain Curves on CFRP Sheets in Beam CB4-2S**

(Refer to Fig. 2 for the location of strain gauges SG1 to SG11, and refer to Table 1 for identification of beam CB4-2S)

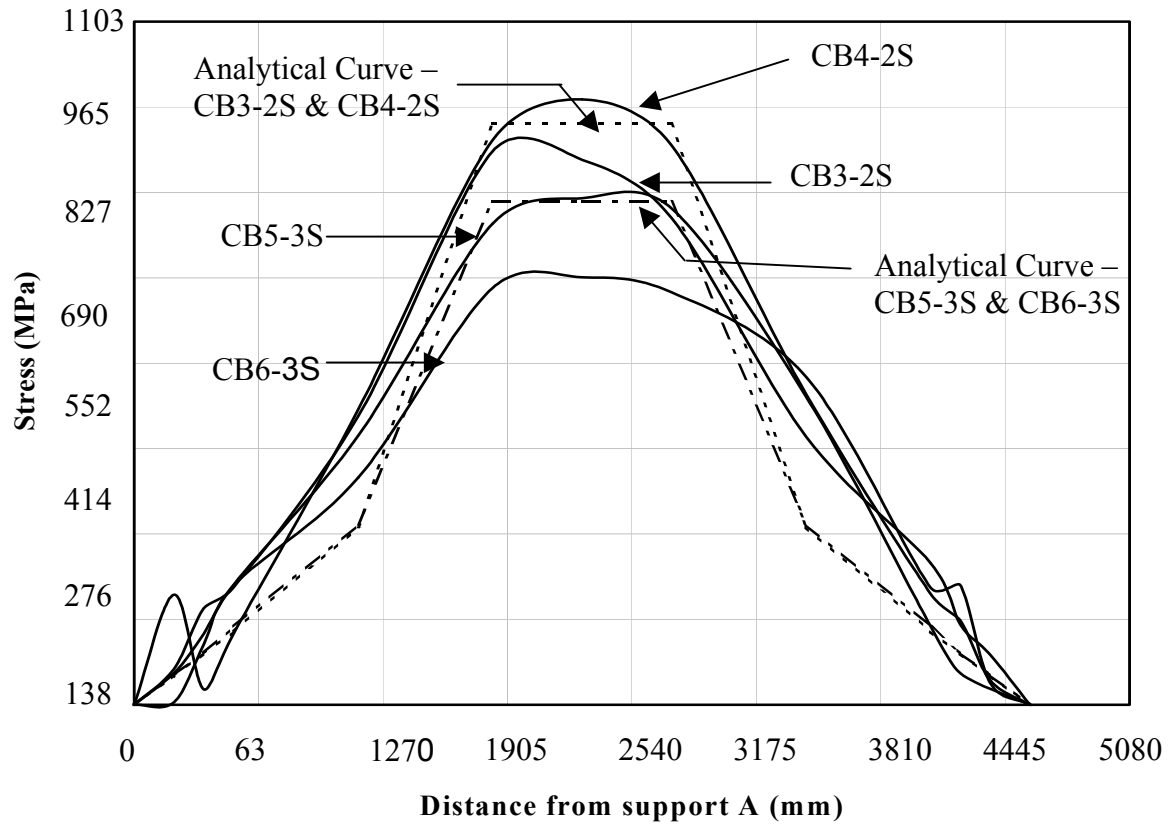


**Figure 9: Longitudinal Stress in 76 mm Wide CFRP Sheets at Failure Load**

(Refer to Table 1 for specimen identification, Table 2 for CFRP sheet properties, and refer to Fig. 1 for location of support A)

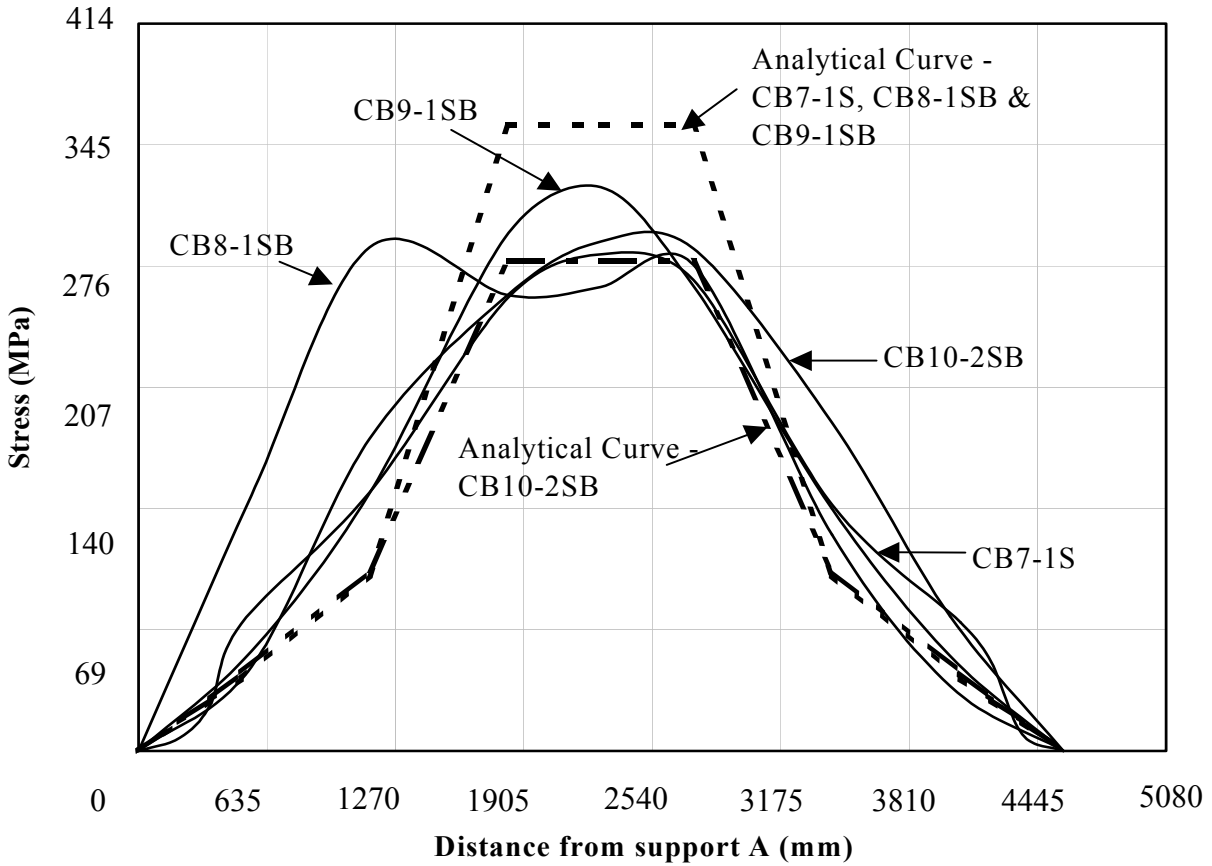


**Figure 10: Longitudinal Stress in 102 mm Wide CFRP Sheets at Failure Load**

(Refer to Table 1 for specimen identification, Table 2 for CFRP sheet properties, and refer to Fig. 1 for the location of support A)

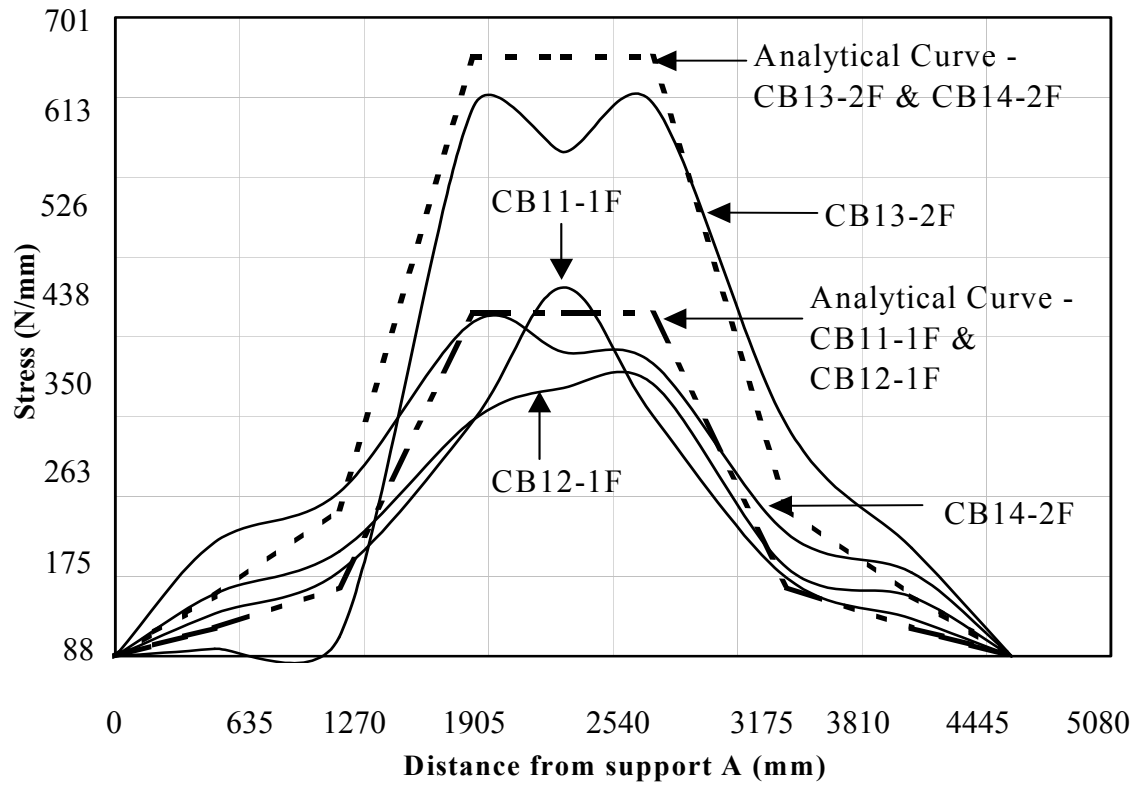
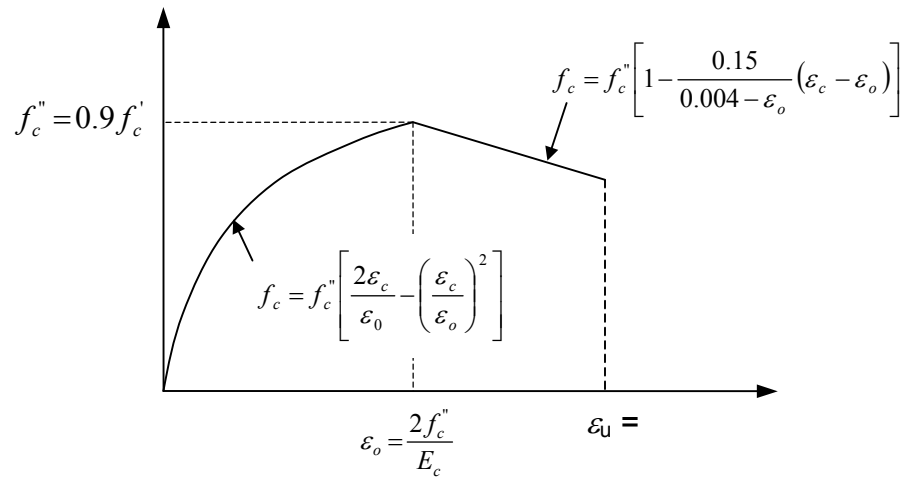
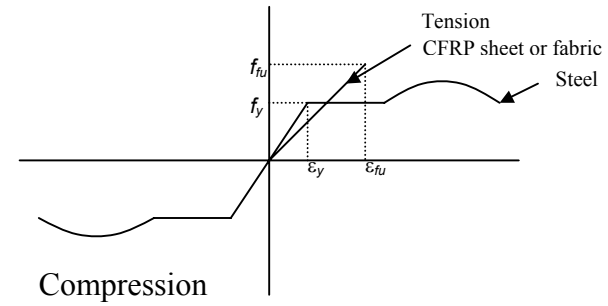


**Figure 11: Longitudinal Stress in CFRP Fabric at Failure Load**

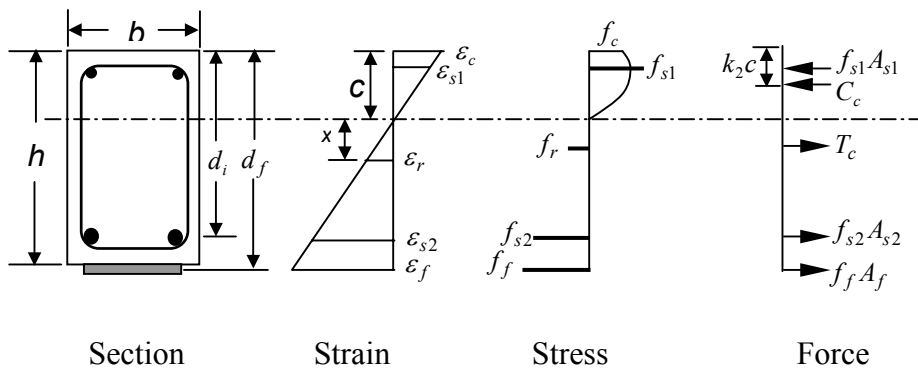
(Refer to Table 1 for specimen identification, Table 2 for CFRP fabric properties,



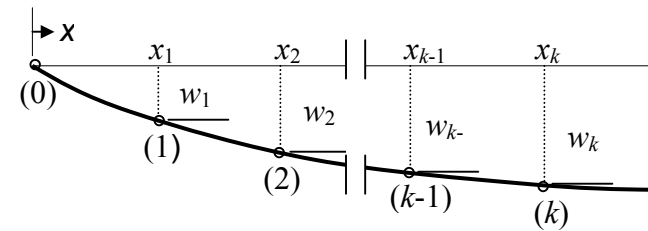
(a)



(b)



(c)



(d)

**Figure 12: (a) Hognestad's Stress-Strain Model for Concrete; (b) Stress-Strain Models for Steel and CFR Sheet/fabric; (c) Strain, Stress, and Force Diagrams; (d) Integration Model for Deflection**

## References

- Alfarabi Sharif, Al-Sulaimani, G.J., Basunbul, I.A., Baluch, M.H., and Ghaleb, B.N. (1994). "Strengthening of initially loaded reinforced concrete beams using FRP plates." *ACI Struct. J.*, 91(2), 160-168.
- Allen Ross, C., David Jerome, M., Joseph Tedesco, W., and Mary Hughes, L. (1999). "Strengthening of reinforced concrete beams with externally bonded composite laminates." *ACI Struct. J.*, 96(2), 212-220.
- Amir Malek, M., Hamid Saadatmanesh, and Mohammad Ehsani, R. (1998). "Prediction of failure load of R/C beams strengthened with FRP plate due to stress concentration at the plate end." *ACI Struct. J.*, 95(2), 142-152.
- Chen, W.F., and Atsuta, T. (1976). *Theory of Beam-Column: Vol. 1 – In-plane Behavior and Design*. McGraw-Hill Book Co., New York, N.Y.
- Edward G. Nawy (1996). *Reinforced concrete*. 3<sup>rd</sup> ed. Prentice Hall, Inc., Englewood Cliffs, New Jersey.
- Grace, N.F., Sayed, G.A., Soliman, A.K., and Saleh, K.R. (1999). "Strengthening reinforced concrete beams using fiber reinforced polymer (FRP) laminates." *ACI Struct. J.*, 96(5), 865-874.
- Hamid Saadatmanesh, and Mohammad Ehsani, R. (1991). "RC beams strengthened with GFRP Plates. I: Experimental study." *J. Struct. Engrg.*, 117(11), 3417-3433.
- Hota GangaRao, V.S. and Vijay, P.V. (1998). "Bending behavior of concrete beams wrapped with carbon fabric." *J. Struct. Engrg.*, 124(1), 3-10.
- Oral Buyukozturk, and Brian Hearing (1998). "Failure behavior of precracked concrete beams retrofitted with FRP." *J. Comp. Const.*, 2(3), 138-144.
- Park, R., and Paulay, T. (1975). *Reinforced concrete structures*. John Wiley and Sons, Inc., New York, N.Y.
- Phalguni Mukhopadhyaya, Narayan Swamy, and Cyril Lynsdale (1998). "Optimizing structural response of beams strengthened with GFRP plates." *J. Comp. Const.*, 2(2), 87-95.
- Rabinovich, O., and Frostig, Y. (2000). "Closed-form high-order analysis of RC beams strengthened with FRP strips." *J. Comp. Const.*, 4(2), 65-74.
- Spadea, G., Bencardino, F., and Swamy, R.N. (1998). "Structural behavior of composite RC beams with externally bonded CFRP." *J. Comp. Const.*, 2(3), 132-137.
- Wei An, Hamid Saadatmanesh, and Mohammad Ehsani, R. (1991). "RC beams strengthened with FRP plates. II: Analysis and parametric study." *J. Struct. Engrg.*, 117(11), 3434-3455.

Yasuhisa Sonobe, Hiroshi Fukuyama, Tadashi Okamoto, et. al. (1997). "Design guidelines of FRP reinforced concrete building structures." *J. Comp. Const.*, 1(3), 90-115.